HHS Public Access

Author manuscript

Circ Res. Author manuscript; available in PMC 2024 August 04.

Published in final edited form as:

Circ Res. 2023 August 04; 133(4): 353–365. doi:10.1161/CIRCRESAHA.122.322337.

Brown Adipose Tissue and BMP3b Decrease Injury in Cardiac Ischemia-Reperfusion

Íngrid Martí-Pàmies[1], **Robrecht Thoonen**[2], **Michael Morley**[1], **Lauren Graves**[1], **Jesus Tamez**[1], **Alex Caplan**[1], **Kendra McDaid**[1], **Vincent Yao**[2], **Allyson Hindle**[3], **Robert E. Gerszten**[4], **Laurie A. Farrell**[4], **Li Li**[1], **Yu-Hua Tseng**[5], **Gerson Profeta**[5], **Emmanuel S Buys**[6], **Donald B Bloch**[6,7], **Marielle Scherrer-Crosbie**[1]

[1]Cardiovascular Institute, Perelman School of Medicine at the University of Pennsylvania, Philadelphia, PA, United States.

[2]Cardiovascular Research Center, Massachusetts General Hospital, Boston, MA, United States.

[3]Anesthesia Center for Critical Care Research, Massachusetts General Hospital, Boston, MA, United States.

[4]Division of Cardiovascular Medicine, Beth Israel Deaconess Medical Center, Boston, MA, United States.

[5]Section on Integrative Physiology and Metabolism, Research Division, Joslin Diabetes Center, Harvard Medical School, Boston, MA, USA

[6]Anesthesia Center for Critical Care Research, Department of Anesthesia, Critical Care and Pain Medicine, Massachusetts General Hospital Research Institute and Harvard Medical School, Boston, MA, United States.

[7]The Center for Immunology and Inflammatory Diseases and the Division of Rheumatology, Allergy and Immunology, Department of Medicine, Massachusetts General Hospital Research Institute and Harvard Medical School, Boston, MA, United States.

Abstract

Background: Despite advances in treatment, myocardial infarction (MI) is a leading cause of heart failure and death worldwide, with both ischemia and reperfusion (I/R) causing cardiac injury. A previous study using a mouse model of non-reperfused MI showed activation of brown adipose tissue (BAT). Recent studies showed that molecules secreted by BAT target the heart. We investigated whether BAT attenuates cardiac injury in I/R, and sought to identify potential cardioprotective proteins secreted by BAT.

Methods: Myocardial I/R surgery with or without BAT transplantation was performed in wild-type (WT) mice and in mice with impaired BAT function (Uncoupling Protein 1 (*Ucp1*)-deficient mice). To identify potential cardioprotective factors produced by BAT, RNAseq was performed

Corresponding author: Marielle Scherrer-Crosbie, marielle.scherrer-crosbie@pennmedicine.upenn.edu, Hospital of the University of Pennsylvania. 11-131, South Pavilion. 3400 Civic Center Blvd. Philadelphia PA 19104. Tel +1 215 662 3569.

Disclosures

None.

in BAT from WT and *Ucp1*$^{-/-}$ mice. Subsequently, myocardial I/R surgery with or without BAT transplantation was performed in Bone Morphogenetic Protein 3b (*Bmp3b*) deficient mice, and WT mice subjected to myocardial I/R were treated using BMP3b.

Results: Dysfunction of BAT in mice was associated with larger MI size after I/R; conversely, augmenting BAT by transplantation decreased MI size. We identified Bmp3b as a protein secreted by BAT after I/R. Compared to WT mice, *Bmp3b*-deficient mice developed larger MIs. Increasing functional BAT by transplanting BAT from WT mice to *Bmp3b*-deficient mice reduced I/R injury whereas transplanting BAT from *Bmp3b*-deficient mice did not. Treatment of WT mice with BMP3b before reperfusion decreased MI size. The cardioprotective effect of BMP3b was mediated through SMAD1/5/8. In humans, the plasma level of BMP3b increased after MI and was positively correlated with the extent of cardiac injury.

Conclusion: The results of this study suggest a cardioprotective role of BAT and of BMP3b, a protein secreted by BAT, in a model of I/R injury. Interventions increasing BMP3b levels or targeting Smad 1/5 may represent novel therapeutic approaches to decrease myocardial damage in I/R injury.

Graphical Abstract

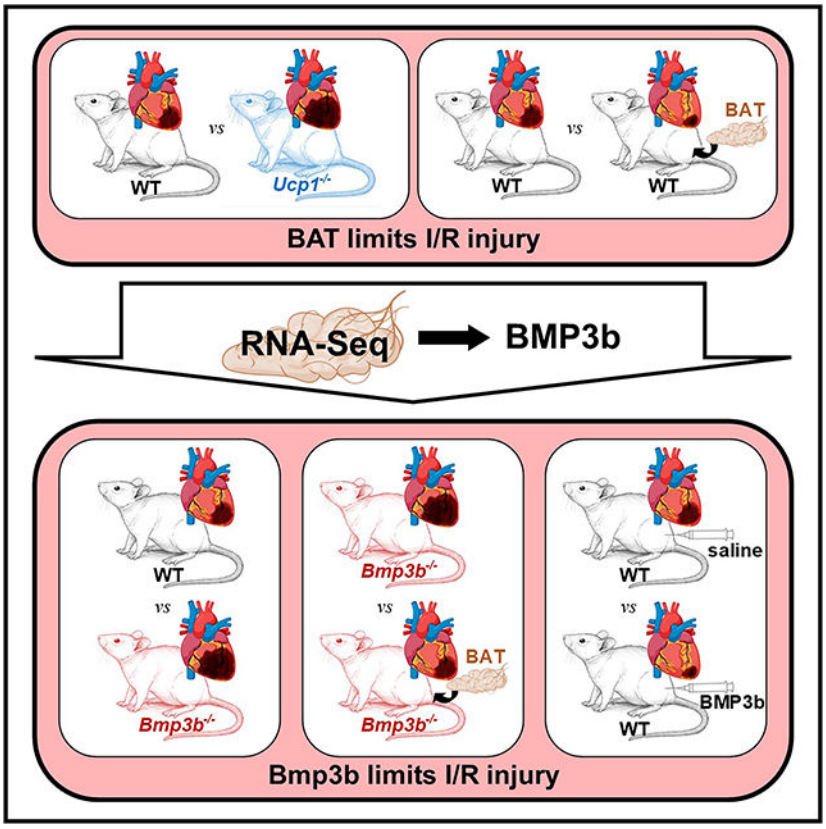

Subject Terms:

Cardiomyopathy; Myocardial Infarction

INTRODUCTION

The incidence of myocardial infarction (MI) approaches fifteen million people worldwide each year. The treatment for MI includes prompt opening of the occluded blood vessel (reperfusion therapy), beta-blockers, and platelet inhibitors. Despite advances in treatment, MI remains a leading cause of heart failure and death (1, 2). A previous study using a mouse model of non-reperfused myocardial infarction and left ventricular (LV) dysfunction showed activation of brown adipose tissue (BAT), which is present in the interscapular region in rodents and the subclavicular region in humans (3). BAT is a major contributor to non-shivering thermogenesis in rodents (4) and has an important role in regulating systemic and cardiac metabolism in mice and humans (5, 6).

The murine model of myocardial ischemia reperfusion (I/R) injury involves temporary occlusion of the left anterior descending (LAD) coronary artery and mimics the clinical situation of a patient with a MI that is promptly reperfused. In this study, we considered the possibilities that the activation of BAT observed in non-reperfused MI occurs in myocardial I/R injury and that BAT has a role in mitigating the extent of myocardial damage.

Brown adipocytes have the capacity to accumulate lipids and take up glucose. The oxidation of glucose and lipids is then uncoupled from ATP production to produce heat. This uncoupling process is driven by the thermogenic protein Uncoupling Protein 1 (UCP1), which is present in BAT mitochondria. Brown adipose tissue is activated by norepinephrine, which is released by the sympathetic nervous system. Norepinephrine activates β-adrenergic receptors in the brown adipocytes, increasing the expression, and triggering the activation, of UCP1 (7). Mice that lack UCP1 have dysfunctional BAT, with impaired thermogenesis, and these mice develop obesity and diabetes (8). Conversely, stimulation of BAT by the sympathetic nervous system increases uptake of triglycerides and normalizes glucose tolerance and insulin resistance in obese mice (9). In addition to these direct metabolic effects, BAT also functions as an endocrine tissue, secreting signaling molecules that target the liver, skeletal muscle, and white adipose tissue (9–12).

Recent studies showed that the molecules secreted by BAT also target the heart. Fibroblast Growth Factor 21 (FGF21), released by BAT when activated by catecholamines, protects against pathologic hypertensive cardiac remodeling (13). The lipokine 12,13-diHOME is also secreted by BAT and reverses cardiac dysfunction and remodeling caused by consumption of a high-fat diet. This lipokine also increased the contractility of isolated cardiomyocytes (14). In previous studies, we showed that increasing the amount of BAT by transplantation decreased cardiac injury and subsequent adverse cardiac remodeling in a catecholamine-induced model of cardiomyopathy (3). The observation that BAT transplantation decreases cardiac injury raises the possibility that BAT may secrete factors that have a direct effect on cardiac injury. In the present study, we report that Bone Morphogenetic Protein 3b (BMP3b) is a cardioprotective factor that is released by BAT in response to myocardial I/R injury.

BMP3b, also known as Growth and Differentiation Factor 10 (GDF10), is a member of the transforming growth factor superfamily. In a mouse model of stroke, treatment with BMP3b

induced neuronal growth and improved recovery (15). In addition, BMP3b enhanced survival in a mouse model of neonatal hypoxia-ischemia-induced encephalopathy (16). Studies from our group using *Bmp3b*-deficient mice revealed that deficiency of BMP3b was associated with progressive weight gain, insulin resistance, and glucose intolerance (17).

In this study, we demonstrate that BAT is activated in cardiac I/R injury and, using a model of BAT transplantation, reveal a cardioprotective role for BAT in limiting the extent of myocardial damage. We identify BMP3b as a cardioprotective protein secreted by BAT after myocardial I/R. Compared to WT mice, *Bmp3b*-deficient mice develop larger MIs, suggesting that BMP3b is necessary to limit MI size. BMP3b treatment, administered prior to ischemia or prior to reperfusion, limits MI size in WT mice. The cardioprotective effect of BMP3b is mediated through BMP second messenger molecules SMAD1/5/8. In humans, the plasma levels of BMP3b increase after MI and are positively correlated with the extent of cardiac injury, as assessed by troponin plasma levels. The results of this study show that in a model of I/R injury, BMP3b, a protein secreted by BAT, has a cardioprotective role. Increasing the level of BMP3b could represent a novel therapeutic approach to ameliorating cardiac I/R injury.

METHODS

Data Availability

The data that support the findings of this study are available from the corresponding authors upon reasonable request.

Please see the extended “Materials and Methods” section and the Major Resources Table in “Supplemental Material” for information and a detailed description of the methodology.

RESULTS

Myocardial ischemia-reperfusion induces Ucp1 expression in BAT and *Ucp1*-deficiency increases ischemia-reperfusion induced myocardial injury.

Myocardial I/R injury activates the sympathetic nervous system and increases the release of natriuretic peptides (18). Because both the sympathetic nervous system and natriuretic peptides increase BAT activity (19), we hypothesized that myocardial I/R would activate BAT. Wild-type (WT) mice were subjected to 45 min of coronary artery ligation or sham thoracotomy followed by 24 hours of reperfusion. Myocardial I/R induced expression of Uncoupling Protein 1 (UCP1) in BAT, as determined by qPCR and immunoblot (Fig 1a–b, Suppl Fig 2), confirming that I/R activates BAT.

Uncoupling protein 1-deficient ($Ucp1^{-/-}$) mice have BAT dysfunction leading to impaired thermogenesis (20, 21). To assess whether BAT dysfunction caused by Ucp1 deficiency is also associated with increased myocardial injury, two month-old $Ucp1^{-/-}$ and WT mice were subjected to myocardial I/R. The MI size was larger in $Ucp1^{-/-}$ mice compared to WT mice, despite the fact that there was no difference in cardiac area-at-risk (AAR) (Fig 1c). In addition, 24 hours after initiation of reperfusion, the plasma levels of cardiac troponin I (cTnI), a measure of myocardial tissue damage, were higher in $Ucp1^{-/-}$ mice than in WT

mice (Fig 1d). These results show that *Ucp1* deletion increases myocardial injury after I/R surgery.

Ucp1$^{-/-}$ mice develop type 2 diabetes at 4 months of age, as indicated by impaired glucose tolerance and increased insulin resistance (22), and diabetes is known to exacerbate myocardial I/R injury (23). We considered the possibility that metabolic abnormalities might contribute to the increased injury observed in the 2-month old *Ucp1*$^{-/-}$ mice used in this study.

However, there was no difference between wild-type and *Ucp1*$^{-/-}$ mice in terms of body weight and fasting levels of glucose and insulin. In addition, there was no difference in the results of glucose and insulin tolerance tests between 2-month old WT and *Ucp1*$^{-/-}$ mice (Suppl Fig1). The results suggest that metabolic changes do not contribute to the increase in I/R injury observed in *Ucp1*$^{-/-}$ mice.

Increasing the level of functional BAT in WT mice limits I/R injury.

Because depletion of functional BAT was associated with increased MI size after I/R injury, we investigated whether increasing the total amount of BAT would decrease the size of MI under the same conditions. BAT from WT mice was transplanted subcutaneously into 7-week-old WT mice and the mice were subjected to myocardial I/R injury 8-weeks later. Immunohistochemistry was used to confirm that the transplanted adipose tissue was viable and functional. Transplanted tissues had similar levels of platelet endothelial cell adhesion molecule 1 (PECAM-1) and tyrosine hydroxylase (TH) as endogenous adipose tissues, suggesting normal vascularization and innervation in the transplanted adipose tissue (24) (Suppl Fig 3a). After myocardial I/R injury, MI size was reduced in mice transplanted with BAT, compared to both sham-transplanted mice and mice that were transplanted with white adipose tissue (WAT) (Fig 2a–b). No differences were observed in the AAR between the three different groups of mice. Furthermore, 24 hours after myocardial I/R injury, cTnI plasma levels were lower in BAT-transplanted mice compared to sham and WAT-transplanted mice (Fig 2c). Thus, increasing the amount of BAT in WT mice decreases myocardial damage after I/R injury.

Increasing the level of BAT might have altered the weight gain and glucose metabolism of transplanted mice, thereby producing the apparent protective effect of BAT transplantation on MI size. To consider this possibility, mice were weighed weekly and glucose tolerance and insulin resistance tests were performed before I/R. Eight weeks after BAT transplantation, there was no difference in body weight, glucose tolerance or insulin resistance in sham-, WAT-, and BAT-transplanted mice (Suppl Fig 3b–d).

Identification of BMP3b as a potential BAT adipokine.

The absence of functional BAT increased myocardial damage in a mouse model of I/R. In contrast, increasing the level of BAT in wild-type mice decreased myocardial damage in this model. To identify potential cardioprotective factors that are produced by BAT, RNAseq was performed on total RNA from BAT isolated from isoproterenol-treated WT and *Ucp1*$^{-/-}$ mice. In these studies, mice were implanted with Alzet minipumps for the infusion of isoproterenol (60 mg/kg/day for 3 days) to activate BAT. WT and *Ucp1*$^{-/-}$ mice with

minipumps infusing saline were used as controls. Gene expression analysis revealed that the activation of BAT in *Ucp1*$^{-/-}$ mice induced a markedly different BAT mRNA profile than the activation of BAT in WT mice, or non-activated BAT in WT or *Ucp1*$^{-/-}$ mice (Fig 3a). The level of mRNA encoding proteins in multiple pathways differed between the activated BAT in WT and *Ucp1*$^{-/-}$ mice, including pathways involved in metabolism, cellular division and growth and protein/peptide secretion (Suppl Fig 4a). As our aim was to explore proteins secreted by activated functional BAT, we focused our interest on the 374 genes upregulated in the isoproterenol-treated WT BAT that did not increase their expression in isoproterenol-treated *Ucp1*$^{-/-}$ BAT (Fig 3b and Suppl Fig 4b). This list was then compared to the UniProt database, resulting in a final set of 30 genes encoding secreted proteins that were increased in the BAT of WT mice but not *Ucp1*$^{-/-}$ mice, after BAT activation (Suppl Table 1). Bone morphogenic protein 3 emerged as a protein of particular interest; Bmp3b has beneficial effects on stroke (15) and survival in a mouse model of neonatal hypoxia-ischemia-induced encephalopathy (16). The increased levels of *Bmp3b* mRNA in isoproterenol-activated BAT in WT compared to *Ucp1*$^{-/-}$ mice were confirmed by qPCR (Fig 3c).

To determine whether myocardial I/R stimulates the synthesis of Bmp3b in BAT, WT mice were subjected to I/R or a sham procedure and the level of mRNA encoding BMP3b and the level of Bmp3b protein were measured. The levels of BMP3b protein and mRNA were statistically higher in the BAT of mice subjected to I/R than in mice in which a sham operation was performed (Fig 3d–e). The plasma levels of Bmp3b were also higher in mice subjected to myocardial I/R compared to sham-treated mice (Fig 3f). These results show that myocardial I/R induces expression of BMP3b in BAT and results in increased BMP3b plasma levels.

Bmp3b-deficiency increases myocardial I/R injury in mice.

To further characterize the potential effect of Bmp3b on myocardial injury, 2-month-old *Bmp3b*-deficient (*Bmp3b*$^{-/-}$) mice were subjected to cardiac I/R. After I/R induced cardiac injury, *Bmp3b*$^{-/-}$ mice developed larger MIs than WT control mice, despite that fact that there were no differences in the size of the AAR (Fig 4a–b). Similarly, plasma troponin cTnI levels were higher in *Bmp3b*$^{-/-}$ mice than in WT mice after 24 hours of reperfusion (Fig 4c). These findings demonstrate that deficiency of Bmp3b increases the extent of cardiac I/R injury.

Increasing functional BAT in *Bmp3b*$^{-/-}$ mice limits I/R injury.

To determine whether the presence of BMP3b is necessary to limit I/R injury, we investigated whether transplantation of BAT, from either WT or *Bmp3b*$^{-/-}$ mice, into *Bmp3b*$^{-/-}$ mice would limit myocardial injury. Three groups of mice were studied: *Bmp3b*$^{-/-}$ mice that received a transplant of BAT from WT mice; *Bmp3b*$^{-/-}$ mice that received a BAT transplant from other *Bmp3b*$^{-/-}$ mice (control #1); or *Bmp3b*$^{-/-}$ mice that underwent a sham transplant procedure (control #2). MI size was decreased in *Bmp3b*$^{-/-}$ mice transplanted with WT BAT compared to *Bmp3b*$^{-/-}$ mice that received a BAT transplant from other *Bmp3b*$^{-/-}$ mice, and *Bmp3b*$^{-/-}$ mice that underwent a sham transplant procedure (Fig 5a–b). There was no difference in myocardial AAR between *Bmp3b*$^{-/-}$ mice transplanted with BAT from WT mice and the two groups of control mice. Plasma cTnI

levels were lower in *Bmp3b*$^{-/-}$ mice transplanted with WT BAT than in control mice (Fig 5c). Immunohistochemical studies showed that all transplanted brown adipose tissue had the expected vascularization and innervation (Suppl Fig 5a). There was no difference in body weight, or glucose or insulin tolerance tests between the three groups of mice (Suppl Fig 5b–d). These findings suggest that WT BAT transplanted to *Bmp3b*$^{-/-}$ mice decreases the I/R-induced myocardial injury observed in *Bmp3b*$^{-/-}$ mice.

BMP3b treatment limits myocardial ischemia-reperfusion injury and apoptosis in WT mice

To directly test whether BMP3b protects against myocardial I/R injury, WT mice were subjected to I/R and treated with BMP3b. Mice were treated with two injections of either BMP3b (10 ng/g body weight) or saline, the first before ligation of the LAD coronary artery and the second just before reperfusion of the LAD. Twenty-four hours after reperfusion, the mice were sacrificed, and the MI size measured. Injection of BMP3b produced a 35% decrease in MI size (Fig 6a). In addition, cTnI plasma levels were lower in mice that were treated with BMP3b than in control mice (Fig 6b).

In clinical practice, it is usually not feasible to administer treatment prior to the onset of a MI. To investigate whether administration of BMP3b at a more clinically-relevant time point might also attenuate myocardial damage, BMP3b was administrated once, but at a higher dose, after the onset of myocardial ischemia but before reperfusion. MI size was smaller in mice treated with BMP3b (50 ng/g body weight) than in control mice that were treated with saline (Fig 6c).

During I/R injury, cardiomyocytes undergo apoptosis (25). To assess the extent of cardiomyocyte apoptosis in mice subjected to I/R reperfusion and treated with BMP3b, hearts were obtained 24 hours after I/R from mice treated with BMP3b before ischemia and before reperfusion. The extent of apoptosis was determined using the TUNEL assay. Compared to control mice that were treated with saline, administration of BMP3b was associated with a smaller number of apoptotic cells in the ischemic area (Fig 6d).

Because BMP3b inhibited apoptosis in mouse hearts after I/R injury, we further investigated the *in vitro* effect of BMP3b on apoptosis in rat neonatal cardiomyocytes (RNCMs). RNCMs were isolated and incubated in serum- and glucose-free media for 24 hours in the presence or absence of BMP3b. In the absence of BMP3b, twenty-four hours of serum/glucose deprivation induced marked apoptosis, as indicated by an increase in caspase activity. In contrast, treatment with BMP3b produced a dose-dependent reduction in caspase activity in serum- and glucose-starved RNCMs (Fig 6e). Taken together, these results demonstrate that treatment with BMP3b limits myocardial injury and decreases apoptosis in I/R injury. BMP3b also decreases apoptosis in serum- and glucose-deprived isolated RNCMs.

The cardioprotective effect of BMP3b in I/R injury is mediated by the phospho-SMAD1/5/8 pathway.

Because BMP3b belongs to the TGF family of proteins, we hypothesized that BMP3b might exert its cardioprotective effects through Type 1 and/or Type 2 BMP receptors (BMPR) and through second messengers SMAD1/5 and/or SMAD2/3. To investigate whether BMP3b

induces phosphorylation of SMAD1/5 after I/R injury *in vivo*, left ventricles were harvested 3 hours after I/R or sham surgery in mice treated with saline or BMP3b. Treatment with BMP3b in mice subjected to I/R was associated with a 6-fold increase in phospho-SMAD1/5 in the LV (Fig 6f). Levels of phospho-SMAD1/5 in the LV were not increased by BMP3b treatment in sham-operated mice nor by I/R surgery in saline-treated mice (Fig 6g).

Levels of phospho-SMAD2/3 were slightly higher in mice that underwent myocardial I/R injury, but pretreatment with BMP3b did not further increase the level of phospho-SMAD2/3 in the LV compared to mice that were pre-treated with saline and exposed to the same surgical procedure (Fig 6g). Thus, BMP3b treatment activates the SMAD1/5 pathway in glucose and serum starved NRCMs and in the LV after a myocardial I/R injury.

Because treatment with Bmp3b increases the level of phospho-SMAD1/5 in the myocardium of I/R injured mice, we investigated whether inhibition of the TGF-β/BMP signaling pathway blocks the effects of BMP3b and increases myocardial injury under the same conditions. WT mice were treated with K02288, a selective inhibitor of Alk1/Alk2/Alk6 receptors (receptors that phosphorylate SMAD1/5), one hour before I/R surgery. Pretreatment with K02288 blocked the cardioprotective effect of BMP3b in mice. Myocardial injury and cTnI plasma levels were similar in mice with I/R surgery that were pretreated with K02288 and subsequently treated with BMP3b as in saline-treated mice (Fig 7a–c). Together, these data suggest that BMP3b treatment limits myocardial injury through phosphorylation of SMAD1/5.

BMP3b plasma levels are increased after myocardial infarction in humans

To determine whether the increase in BMP3b plasma levels observed in mice after I/R surgery is also present in humans experiencing myocardial damage, BMP3b was measured in plasma samples from patients undergoing alcohol septal ablation (22 patients including 11 men, 62±2 years old, BMI 35±2 kg/m^2). This technique, used in patients with hypertrophic cardiomyopathy, induces a controlled infarction of the hypertrophied septum (26). Plasma levels of BMP3b, measured by ELISA, increased one hour after the intervention (Fig 8a). BMP3b plasma levels were positively correlated with MI size as assessed by troponin I levels measured 24 hours after septal ablation (Fig 8b).

DISCUSSION

In this study, we report that BAT is activated after I/R in mice, genetic ablation of BAT is associated with increased I/R induced myocardial injury, and increasing the level of functional BAT in WT mice limits I/R injury. We identify BMP3b as a potential cardioprotective BAT adipokine. *Bmp3b*-deficiency increases myocardial I/R injury in mice. Increasing the amount of functional BAT in *Bmp3b*$^{-/-}$ mice limits I/R injury, whereas increasing the amount of BAT that lacks BMP3b has no effect. Infusion of BMP3b limits myocardial I/R injury and apoptosis in WT mice. The cardioprotective effect of BMP3b in I/R injury is mediated by the SMAD1/5/8 pathway. In humans, BMP3b plasma levels are increased after MI and higher levels of BMP3b are associated with higher levels of troponin.

Numerous studies in rodents and humans have demonstrated the beneficial effects of BAT on glucose and lipid metabolism (24, 27, 28). Recently, the presence of BAT in humans was also reported to be associated with a decrease in the prevalence of coronary artery disease and heart failure (29). Several studies reported a decrease in glucose levels and an increase in insulin sensitivity after BAT transplantation in mice (24, 30, 31); however, these experiments were conducted in diabetic or obese animals, and the effects were found several months after BAT transplantation. In this study, we extend these findings by showing that increasing the amount of BAT through transplantation in mice has a direct effect on myocardial I/R, independent of its effect on systemic metabolism.

To evaluate the effects of a decrease in functional BAT on I/R injury, we subjected *Ucp1*$^{-/-}$ mice to I/R surgery. Although investigators have used surgical removal of interscapular BAT to study the acute effect of BAT ablation, the rapid compensatory growth of other BAT depots would confound the study of a subsequent I/R injury (32). However, mice that are deficient in UCP1 had defective thermogenesis and dysfunctional BAT. The importance of functional BAT in decreasing I/R injury is emphasized by the greater injury after I/R sustained by *Ucp1*$^{-/-}$ mice, which is independent of metabolic changes. To mimic the thermoneutral conditions in which humans live, mice were maintained at thermoneutrality on the day of the procedure. Whether a colder environment would elicit a greater difference between WT and *Ucp1*$^{-/-}$ mice due to BAT activation in both strains. A limitation of using *Ucp1*$^{-/-}$ mice as a model of impaired BAT must be noted: the hearts of cardiac-specific *Ucp1* transgenic mice have improved functional recovery after global ischemia compared to the hearts of their wild-type counterparts (33). Moreover, a recent study in rats has suggested that *Ucp1* deficiency exacerbates isoproterenol-induced myocardial injury by inhibition of protective AMPK/mTOR/PPARα signaling in the heart (34). Thus, a direct protective effect of Ucp1 expressed in the myocardium cannot be excluded in these experiments.

The finding that BAT transplantation decreases myocardial I/R injury, independent of an effect on systemic metabolism, raises the possibility that BAT exerts an effect on the heart through its endocrine properties (3, 35, 36). We used RNA sequencing of isoproterenol-activated BAT to identify potential cardioprotective proteins secreted by BAT in WT mice, but not in *Ucp1*$^{-/-}$ mice. The BAT transcriptome of *Ucp1*$^{-/-}$ mice differed markedly from that of WT mice after isoproterenol activation, including altered expression of genes involved in cellular division and apoptosis. These results are similar to those of Maurer *et al.* who analyzed the transcriptome of BAT in WT and *Ucp1*$^{-/-}$ after 4 weeks at thermoneutrality or mild cold exposure (20°C) and reporting impaired adaptation to thermogenic stimulation at the level of tissue growth and metabolic turnover of substrates (37). Interestingly, previous work illustrated that after 3 weeks of exposure to mild cold and a high fat diet, the synthesis and secretion of fibroblast growth factor (FGF) 21, a cardioprotective factor, is increased in the BAT of *Ucp1*$^{-/-}$ mice compared to the BAT of WT mice (38). Similarly, we noted an increase in the synthesis of FGF21 in the BAT of *Ucp1*$^{-/-}$ mice compared to the BAT of WT mice after 3 days of isoproterenol exposure. Therefore, *Ucp1*-deficiency is associated with changes in the synthesis of multiple proteins in BAT. Additionally, the increased synthesis of FGF21 in the activated BAT of *Ucp1*$^{-/-}$ mice rules out FGF21 as the mediator of cardioprotection in the current model of I/R.

We focused on BMP3b, a member of the TGFβ family that has a neuroprotective effect after stroke (15), and promotes regeneration in several types of cells, including axonal sprouting in neurons after ischemia (15) and growth in aging muscle cells (39). Compared to WT mice, *Bmp3b*-deficient mice develop glucose intolerance and insulin resistance at 6-month of age (17). In studies comparing 2-month-old *Bmp3b*-deficient mice with age-matched WT mice, no metabolic abnormalities or baseline differences in cardiac function were detected (17). Despite this preserved metabolic and cardiac phenotype, the absence of Bmp3b was associated with greater MI size after I/R.

Importantly, BMP3b treatment administered before I/R and shortly before reperfusion limited MI size. BAT transplantation from WT mice into *Bmp3b*$^{-/-}$ mice limited MI size whereas BAT transplantation from *Bmp3b*$^{-/-}$ mice into *Bmp3b*$^{-/-}$ mice did not have a similar effect, emphasizing that the presence of BMP3b is required for the cardioprotective effects of BAT transplantation. This finding could suggest that BMP3b in BAT is required; alternatively, as previously shown by our team, mice deficient in Bmp3b have abnormal BAT at 6-month-old, but there were no differences in the BAT mass or cell morphology by hematoxylin-eosin staining between WT and *Bmp3b*$^{-/-}$ 2-month-old mice. Furthermore, there were no differences in the insulin tolerance test, glucose tolerance test, cholesterol, triglycerides, and HDL plasma levels, suggesting that BAT function was also similar between WT and *Bmp3b*$^{-/-}$ mice at this age (17).

The pathway mediating the regenerative effect of BMP3b may be different between cell types; in primary neurons after ischemia, knockdown of SMAD2 or SMAD3 significantly inhibited the axonal outgrowth effect of BMP3b whereas knockdown of SMAD1 or 5 did not, suggesting axonal sprouting is mediated through SMAD2/3 (15). In contrast, the SMAD1/5/8 pathway was attenuated in the atrophied striated muscle of *Bmp3b*$^{-/-}$ mice and conversely, activation of SMAD1/5/8, but not SMAD2/3 was noted when human myotubes were treated with BMP3b (39). However, the receptors responsible for the BMP3b signal transduction to the different cells have not yet been defined. In the present study, the cardioprotective effect of BMP3b was mediated by SMAD1/5, and involved a decrease in apoptosis, both *in vivo* and in isolated cardiomyocytes. The observed decrease in apoptosis is concordant with results observed in SMAD1 transfection of isolated cardiomyocytes and in SMAD1-transgenic mice subjected to I/R (40).

The plasma levels of BMP3b increased in humans after alcohol septal ablation and correlated with the extent of the MI, suggesting that BMP3b secretion increases as a compensatory factor to myocardial injury. Alcohol septal ablation was chosen because this procedure allowed comparisons in individual patients before and after MI. It is important to note however that the size of the alcohol-induced MI is small and the levels of troponin were within a limited range, between 0.6 and 4 ng/ml. Larger studies with a wider range of MI size are warranted to understand the role of BMP3b in the response to I/R in humans.

In summary, BAT has a cardioprotective role in myocardial I/R injury in mice. We identify BMP3b as a cardioprotective protein secreted by BAT after myocardial I/R injury. BMP3b is necessary to limit I/R injury, and treatment with BMP3b decreases MI size after I/R in mice.

BMP3b also increases after MI in human subjects and BMP3b plasma levels are correlated with the magnitude of myocardial injury.

In the past decades, the diagnosis and treatment of MI has notably improved with mechanical and pharmacological interventions to treat myocardial ischemia. The use of adjunctive pharmacological treatments, potentially able to limit MI size and apoptosis during reperfusion, is still an important research field to reduce long-term mortality. Our findings suggest that BMP3b and SMAD1/5 may be targeted to decrease myocardial damage in I/R injury.

Supplementary Material

Refer to Web version on PubMed Central for supplementary material.

Acknowledgments

The cardiac surgeries were performed by the Mouse Cardiovascular Phenotyping Core at the University of Pennsylvania supported by the Penn Cardiovascular Institute. The IHC were performed by the Histology and Gene Expression Co-Op Core at the University of Pennsylvania.

Sources of Funding

This work was supported by the NIH (R01HL131613 to MS-C) and the Luisa Hunnewell, Larry Newman and The Feil Family Foundation (to DBB).

NON-STANDARD ABBREVIATIONS AND ACRONYMS

AAR	Area at Risk
BAT	Brown adipose tissue
BMP3b	Bone Morphogenetic Protein 3b
I/R	Ischemia/Reperfusion
LAD	Left anterior descending
LV	Left ventricle
MI	Myocardial infarction
NRCM	Neonatal Rat Cardiomyocytes
UCP1	Uncoupling Protein 1
WAT	White adipose tissue
WT	Wild-type

REFERENCES

1. Nascimento BR, Brant LCC, Marino BCA, Passaglia LG, Ribeiro ALP. Implementing myocardial infarction systems of care in low/middle-income countries. Heart 2019;105(1):20–26. [PubMed: 30269080]

2. Virani SS et al. Heart Disease and Stroke Statistics—2021 Update. Circulation 2021;143:E254–E743. [PubMed: 33501848]

3. Thoonen R et al. Functional brown adipose tissue limits cardiomyocyte injury and adverse remodeling in catecholamine-induced cardiomyopathy. J Mol Cell Cardiol 2015;84:202–211. [PubMed: 25968336]

4. Saito M, Matsushita M, Yoneshiro T, Okamatsu-Ogura Y. Brown Adipose Tissue, Diet-Induced Thermogenesis, and Thermogenic Food Ingredients: From Mice to Men. Front Endocrinol (Lausanne) 2020;11.

5. Yang FT, Stanford KI. Batokines: Mediators of Inter-Tissue Communication (a Mini-Review). Curr Obes Rep 2022;11:1–9. [PubMed: 34997461]

6. Gavaldà-Navarro A, Villarroya J, Cereijo R, Giralt M, Villarroya F. The endocrine role of brown adipose tissue: An update on actors and actions. Rev Endocr Metab Disord 2021;23(1):31–41. [PubMed: 33712997]

7. McNeill BT, Suchacki KJ, Stimson RH. MECHANISMS IN ENDOCRINOLOGY: Human brown adipose tissue as a therapeutic target: warming up or cooling down?. Eur J Endocrinol 2021;184(6):R243–R259. [PubMed: 33729178]

8. Feldmann HM, Golozoubova V, Cannon B, Nedergaard J. UCP1 ablation induces obesity and abolishes diet-induced thermogenesis in mice exempt from thermal stress by living at thermoneutrality. Cell Metab 2009;9(2):203–209. [PubMed: 19187776]

9. Bartelt A et al. Brown adipose tissue activity controls triglyceride clearance. Nat Med 2011;17(2):200–206. [PubMed: 21258337]

10. Wang GX et al. The brown fat-enriched secreted factor Nrg4 preserves metabolic homeostasis through attenuation of hepatic lipogenesis. Nat Med 2014;20(12):1436–1443. [PubMed: 25401691]

11. Kong X et al. Brown Adipose Tissue Controls Skeletal Muscle Function via the Secretion of Myostatin. Cell Metab 2018;28(4):631–643.e3. [PubMed: 30078553]

12. Cereijo R et al. CXCL14, a Brown Adipokine that Mediates Brown-Fat-to-Macrophage Communication in Thermogenic Adaptation. Cell Metab 2018;28(5):750–763.e6. [PubMed: 30122557]

13. Ruan CC et al. A 2A Receptor Activation Attenuates Hypertensive Cardiac Remodeling via Promoting Brown Adipose Tissue-Derived FGF21. Cell Metab 2018;28(3):476–489.e5. [PubMed: 30017353]

14. Pinckard KM et al. A Novel Endocrine Role for the BAT-Released Lipokine 12,13-diHOME to Mediate Cardiac Function. Circulation 2021;145–159. [PubMed: 33106031]

15. Li S et al. GDF10 is a signal for axonal sprouting and functional recovery after stroke. Nat Neurosci 2015;18(12):1737–45. [PubMed: 26502261]

16. Ogawa Y, Tsuji M, Tanaka E, Miyazato M, Hino J. Bone Morphogenetic Protein (BMP)-3b Gene Depletion Causes High Mortality in a Mouse Model of Neonatal Hypoxic-Ischemic Encephalopathy. Front Neurol 2018;9:397. [PubMed: 29922215]

17. Martí-Pàmies Í et al. Deficiency of bone morphogenetic protein-3b induces metabolic syndrome and increases adipogenesis. American Journal of Physiology-Endocrinology and Metabolism 2020;319(2):E363–E375. [PubMed: 32603262]

18. Nishikimi T, Maeda N, Matsuoka H. The role of natriuretic peptides in cardioprotection. Cardiovasc Res 2006;69(2):318–328. [PubMed: 16289003]

19. Thoonen R, Hindle AG, Scherrer-Crosbie M. Brown adipose tissue: The heat is on the heart. Am J Physiol Heart Circ Physiol 2016;310(11):H1592–H1605. [PubMed: 27084389]

20. Golozoubova V, Cannon B, Nedergaard J. UCP1 is essential for adaptive adrenergic nonshivering thermogenesis. Am J Physiol Endocrinol Metab 2006;291(2).

21. Ikeda K et al. UCP1-independent signaling involving SERCA2b-mediated calcium cycling regulates beige fat thermogenesis and systemic glucose homeostasis. Nat Med 2017;23(12):1454–1465. [PubMed: 29131158]

22. Thoonen R et al. Brown Adipocyte Dysfunction in UCP1 Knockout Mice leads to Age-Dependent Development of Type 2 Diabetes. The FASEB Journal 2015;29(S1):995.13.

23. Paulson DJ. The diabetic heart is more sensitive to ischemic injury. Cardiovasc Res 1997;34(1):104–112. [PubMed: 9217879]
24. Stanford KI et al. Brown adipose tissue regulates glucose homeostasis and insulin sensitivity. Journal of Clinical Investigation 2013;123(1):215–223. [PubMed: 23221344]
25. Davidson SM et al. Mitochondrial and mitochondrial-independent pathways of myocardial cell death during ischaemia and reperfusion injury. J Cell Mol Med 2020;24(7):3795–3806. [PubMed: 32155321]
26. Rigopoulos AG, Panou F, Kremastinos DT, Seggewiss H. Alcohol Septal Ablation for Hypertrophic Obstructive Cardiomyopathy. Curr Cardiol Rev 2008;4(3):193. [PubMed: 19936195]
27. Chondronikola M et al. Brown Adipose Tissue Activation Is Linked to Distinct Systemic Effects on Lipid Metabolism in Humans. Cell Metab 2016;23(6):1200–1206. [PubMed: 27238638]
28. Gunawardana SC, Piston DW. Insulin-independent reversal of type 1 diabetes in nonobese diabetic mice with brown adipose tissue transplant. Am J Physiol Endocrinol Metab 2015;308(12):E1043–E1055. [PubMed: 25898954]
29. Becher T et al. Brown adipose tissue is associated with cardiometabolic health. Nature Medicine 2021 27:1 2021;27(1):58–65.
30. Liu X et al. Brown adipose tissue transplantation improves whole-body energy metabolism. Cell Research 2013 23:6 2013;23(6):851–854.
31. Liu X et al. Brown Adipose Tissue Transplantation Reverses Obesity in Ob/Ob Mice. Endocrinology 2015;156(7):2461–2469. [PubMed: 25830704]
32. Rothwell NJ, Stock MJ. Surgical removal of brown fat results in rapid and complete compensation by other depots. American Journal of Physiology 1989;257(2):R253–8. [PubMed: 2548406]
33. Hoerter J et al. Mitochondrial uncoupling protein 1 expressed in the heart of transgenic mice protects against ischemic-reperfusion damage. Circulation 2004;110(5):528–533. [PubMed: 15262832]
34. Hou D et al. Uncoupling protein 1 knockout aggravates isoproterenol-induced acute myocardial ischemia via AMPK/mTOR/PPARα pathways in rats. Transgenic Res 2022;31(1):107–118. [PubMed: 34709566]
35. Ferrer-Curriu G et al. Fibroblast growth factor-21 protects against fibrosis in hypertensive heart disease. J Pathol 2019;248(1):30–40. [PubMed: 30582148]
36. Planavila A et al. Fibroblast growth factor 21 protects against cardiac hypertrophy in mice. Nat Commun 2013;4.
37. Maurer SF, Fromme T, Mocek S, Zimmermann A, Klingenspor M. Uncoupling protein 1 and the capacity for nonshivering thermogenesis are components of the glucose homeostatic system. Am J Physiol Endocrinol Metab 2020;318(2):E198–E215. [PubMed: 31714796]
38. Keipert S et al. Endogenous FGF21-signaling controls paradoxical obesity resistance of UCP1-deficient mice. Nature Communications 2020 11:1 2020;11(1):1–12.
39. Uezumi A et al. Mesenchymal Bmp3b expression maintains skeletal muscle integrity and decreases in age-related sarcopenia. J Clin Invest 2021;131(1).
40. Masaki M et al. Smad1 protects cardiomyocytes from ischemia-reperfusion injury. Circulation 2005;111(21):2752–2759. [PubMed: 15911698]
41. Zhao R, Lawler AM, Lee S-J. Characterization of GDF-10 Expression Patterns and Null Mice. Dev Biol 1999;212(1):68–79. [PubMed: 10419686]
42. Kaikaew K, Grefhorst A, Visser JA. Sex Differences in Brown Adipose Tissue Function: Sex Hormones, Glucocorticoids, and Their Crosstalk. Front Endocrinol (Lausanne) 2021;12.
43. Dobin A et al. STAR: ultrafast universal RNA-seq aligner. Bioinformatics 2013;29(1):15–21. [PubMed: 23104886]
44. Ritchie ME et al. limma powers differential expression analyses for RNA-sequencing and microarray studies. Nucleic Acids Res 2015;43(7):e47. [PubMed: 25605792]
45. Leek JT, Johnson WE, Parker HS, Jaffe AE, Storey JD. The sva package for removing batch effects and other unwanted variation in high-throughput experiments. Bioinformatics 2012;28(6):882–883. [PubMed: 22257669]

46. Wu T et al. clusterProfiler 4.0: A universal enrichment tool for interpreting omics data. Innovation (Cambridge (Mass.)) 2021;2(3).

NOVELTY AND SIGNIFICANCE

What is known?

- Brown adipose tissue (BAT), known to increase thermogenesis, also functions as an endocrine tissue.
- Increasing the amount of BAT by transplantation decreases cardiac injury in a catecholamine-induced model of cardiomyopathy.
- Bone morphogenetic protein 3 (BMP3b also known as GDF10), a protein secreted by BAT, induces neuronal growth and improves recovery in murine brain infarction.

What new information does this article contribute?

- Increasing the amount of BAT in wild-type mice by BAT transplantation decreases cardiac injury after cardiac ischemia/reperfusion (I/R).
- BMP3b, a protein secreted by BAT, is cardioprotective in cardiac I/R

The observation that BAT transplantation decreases cardiac injury in catecholamine-induced cardiomyopathy raises the possibility that BAT may secrete factors that have a direct effect on cardiac injury. We demonstrate that BAT is activated in cardiac I/R injury and, using a model of BAT transplantation, reveal a cardioprotective role for BAT in limiting the extent of myocardial damage. We identify BMP3b as a cardioprotective protein secreted by BAT after myocardial I/R. Compared to wild-type mice, *Bmp3b*-deficient mice develop larger myocardial infarctions after I/R suggesting that BMP3b is necessary to limit MI size. Additionally, BMP3b treatment, administered prior to ischemia or prior to reperfusion, limits MI size in wild-type mice. The cardioprotective effect of BMP3b is mediated through BMP second messenger molecules SMAD1/5/8. In humans, the plasma levels of BMP3b increase after myocardial infarction and are positively correlated with the extent of cardiac injury, as assessed by troponin plasma levels. The results of this study show that in a model of I/R injury, BMP3b, a protein secreted by BAT, has a cardioprotective role. Increasing the level of BMP3b could represent a novel therapeutic approach to ameliorating cardiac I/R injury.

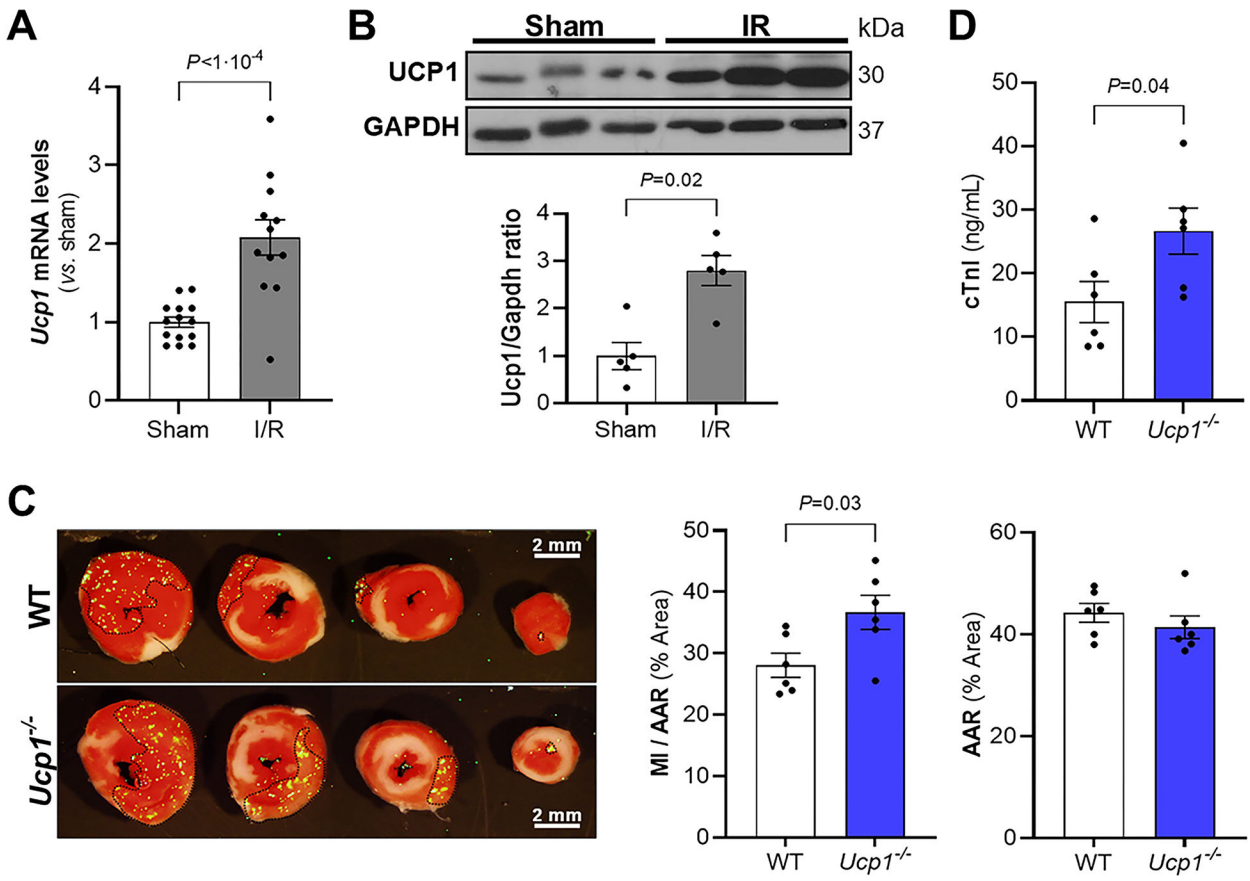

Figure 1. BAT is activated by myocardial I/R and *Ucp1*-deficiency increases myocardial injury after I/R.

Wild-type mice were subjected to myocardial I/R or to a sham procedure. BAT was isolated, the level of *Ucp1* mRNA was measured using real time qPCR (*A*, Sham, $n = 14$; I/R, $n = 12$) and the levels of Ucp1 protein were determined by immunoblot (*B*, $n = 5$ mice for each condition). Gapdh was used as a loading control. In the lower panel of *B*, the graph shows the densitometric analysis of Western blots. Values expressed as means ± SE. $*P < 0.05$ vs. sham. *C*) Representative images of Triphenyltetrazolium chloride (TTC) staining and fluorescent microspheres distribution (green dots) of myocardial sections from WT and *Ucp1*$^{-/-}$ mice 24 h after reperfusion. The viable non-ischemic area is shown in green dots and delineated with black dotted line; the ischemic area (area at risk, AAR) is the region without green dots; and the infarcted area (myocardial infarction, MI), appears in white. The MI area and the AAR from each section were measured using Image J. The ratio of MI area to AAR (MI/AAR) and AAR are shown (*right side of panel C*, $n = 6$ mice for each condition). Values expressed as means ± SE. $*P < 0.05$ *vs.* WT. *D*) The level of cardiac troponin I (cTnI) was measured 24 h after reperfusion injury in WT and *Ucp1*$^{-/-}$ mice. ($n = 6$ mice for each condition). Values expressed as means ± SE. $*P < 0.05$ *vs.* WT. *P* values were determined by unpaired Student *t*-test (*A, C* and *D*) and Mann-Whitney test (*B*).

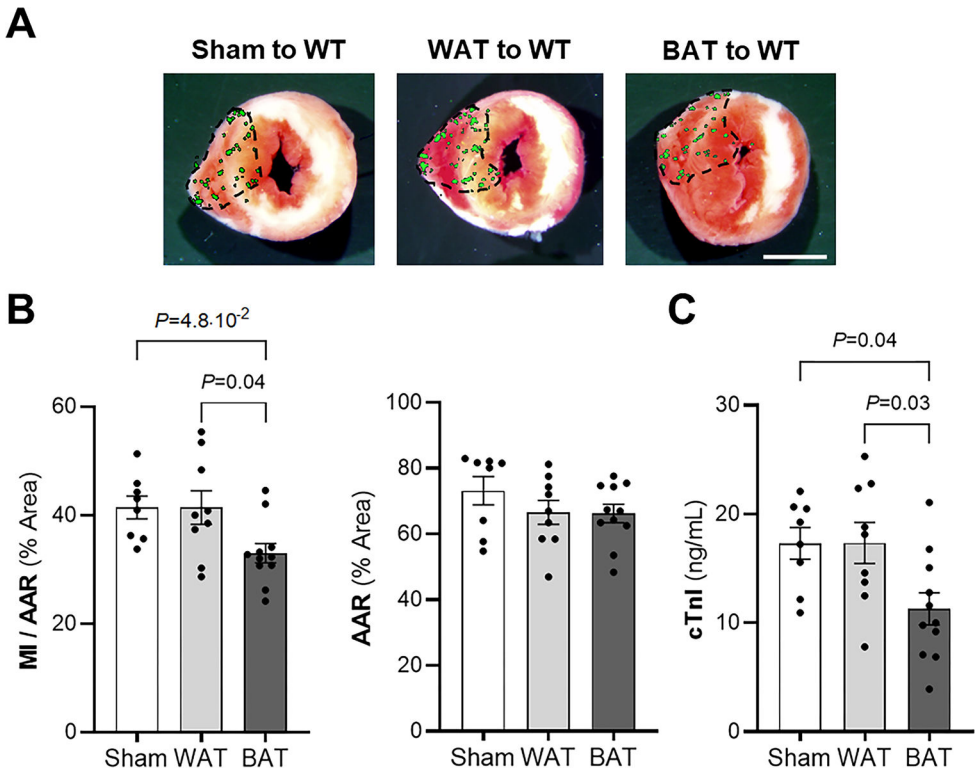

Figure 2. Increasing functional brown adipose tissue (BAT) in WT mice limits I/R injury.

Wild-type (WT) mice received BAT transplant, white adipose tissue (WAT) transplant (both from WT mice donors) or underwent a sham procedure. Representative images (*A*) and quantitative analysis *(B)* of Triphenyltetrazolium chloride (TTC) staining of myocardial infarction (MI) to area-at-risk (AAR) (MI/AAR) and AAR. The MI/AAR and AAR were measured after 45 min of ischemia and 24 h of reperfusion. (Sham, $n = 8$; WAT, $n = 9$; BAT, $n = 11$). Values are means ± SE. Scale bar: 2 mm. *C*) The level of cardiac troponin I (cTnI) was measured in plasma by ELISA 24 h after ischemia-reperfusion injury in sham, WAT and BAT transplant to WT mice. (Sham, $n = 8$; WAT, $n = 9$; BAT, $n = 11$). Values expressed as means ± SE. *P* values were determined by one-way ANOVA with Tukey correction (*B* and *C*).

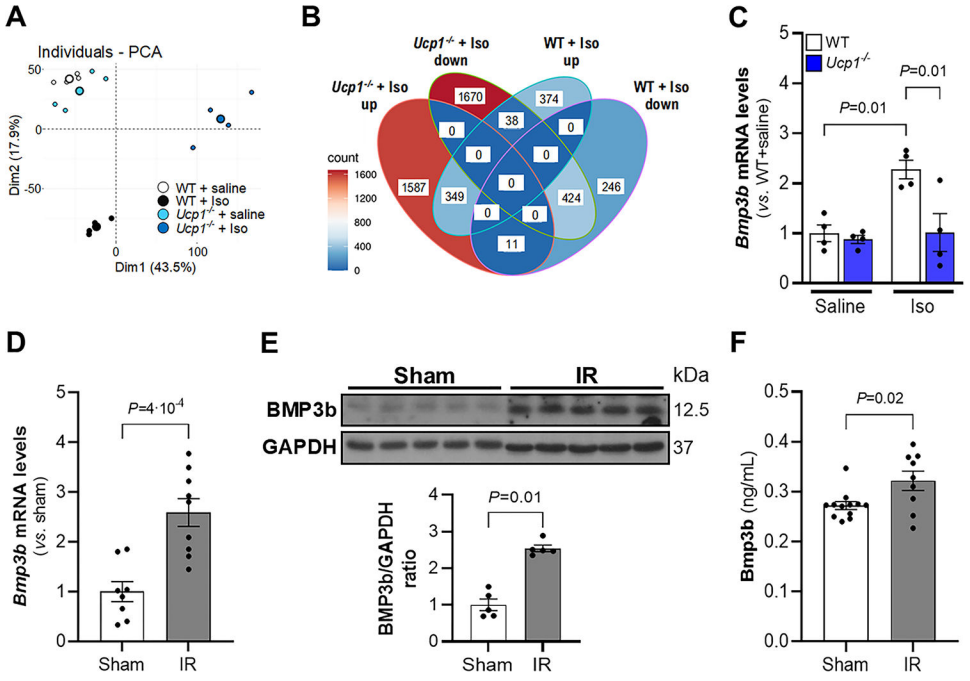

Figure 3. Identification of BMP3b as a potential BAT adipokine using RNA-Seq.

A) Principal component analysis (PCA) of RNA-Seq data from WT and *Ucp1*$^{-/-}$ treated with saline or isoproterenol (Iso) during 3 days (60 mg/kg/day). Each small point represents an RNA-Seq sample ($n = 4$), and bigger points represent the average of the group data for each condition. *B*) Venn diagram of differentially expressed genes increased (up) or decreased (down) by isoproterenol (Iso) treatment in comparison to saline treatment in WT and *Ucp1*$^{-/-}$ mice. *C*) Gene expression of *Bmp3b* was assessed by real-time PCR in BAT in WT and *Ucp1*$^{-/-}$ mice after saline or isoproterenol (Iso) infusion for 3 days ($n = 4$ in each group). Values are means ± SE. *Bmp3b* was assessed by real-time PCR (*D*) and by Western blot (*E*) in BAT 24 h after sham or myocardial ischemia-reperfusion (IR) surgery in WT mice (real-time PCR: Sham, $n = 8$; IR, $n = 9$; Western blot: $n = 5$ each group). Results are expressed as means ± SE. *F*) Bmp3b plasma levels were quantified by ELISA 24 h after sham or myocardial ischemia-reperfusion (IR) surgery in WT mice (Sham, $n = 12$; IR, $n = 9$;). Results are expressed as means ± SE. *P* values were determined by unpaired Student *t*-test (*D* and *F*) and Mann-Whitney test. (*B*) Normality was assessed by Shapiro-Wilk test and *P* values were determined by two-way ANOVA with Tukey correction.

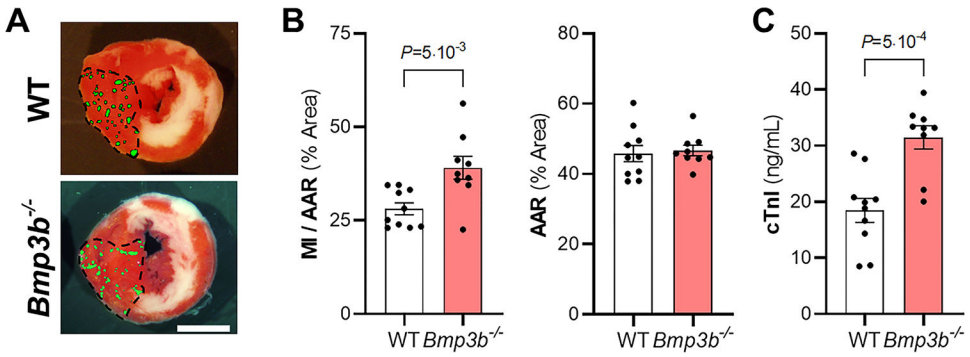

Figure 4. *Bmp3b* deficiency in mice increases myocardial I/R injury.

WT and *Bmp3b*$^{-/-}$ mice were subjected to myocardial I/R injury. *A*) Representative images of Triphenyltetrazolium chloride (TTC) staining and fluorescent microsphere distribution (green dots) of myocardial sections 24 h after reperfusion. Scale bar: 2 mm. *B*) Myocardial infarction (MI) to area-at-risk (AAR) (MI/AAR) and AAR were measured after 45 min ischemia and 24 h reperfusion (WT, $n = 10$; *Bmp3b*$^{-/-}$, $n = 9$). Values are means ± SE. *C*) The level of cardiac troponin I (cTnI) was measured in plasma by ELISA 24 h after I/R injury in WT and *Bmp3b*$^{-/-}$ mice (WT, $n = 10$; *Bmp3b*$^{-/-}$, $n = 9$). Values expressed as means ± SE. *P* values were determined by unpaired Student *t*-test (*B* and *C*).

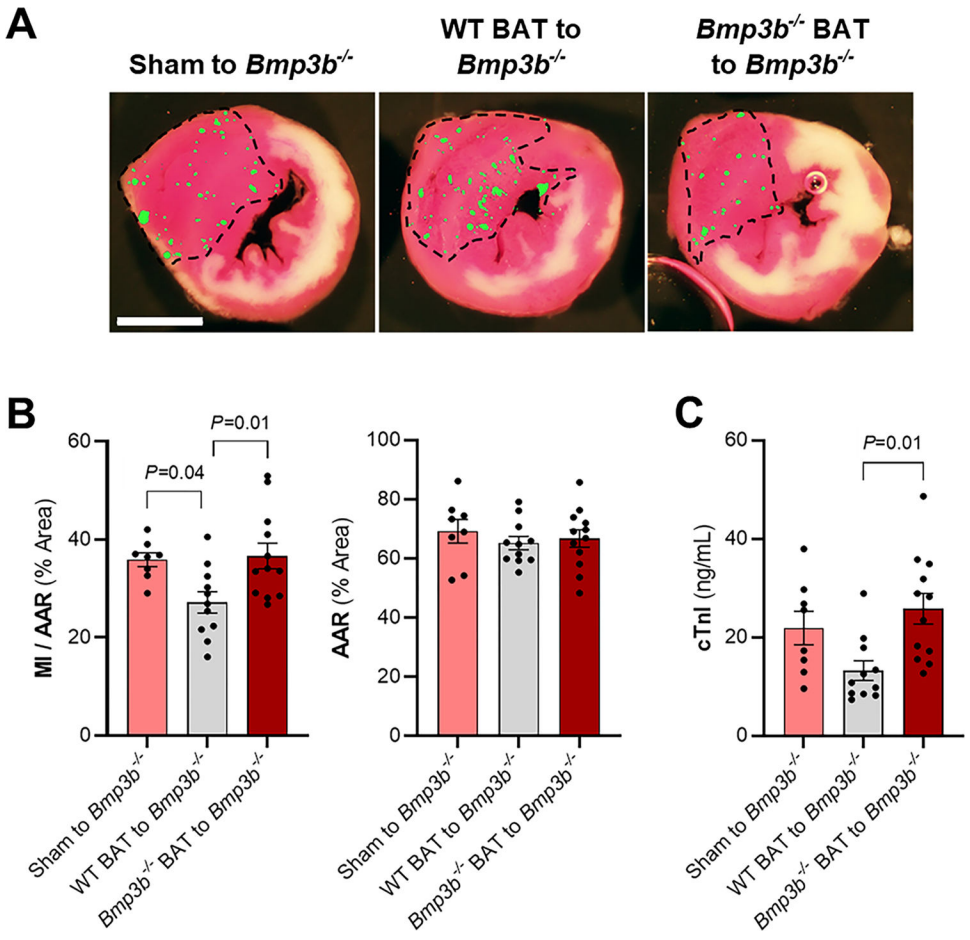

Figure 5. Restoring functional brown adipose tissue (BAT) in *Bmp3b*$^{-/-}$ mice decreases myocardial I/R injury.

Bmp3b$^{-/-}$ mice received BAT transplant from *Bmp3b*$^{-/-}$ mice, from WT mice, or underwent a sham procedure. *A*) Representative images of Triphenyltetrazolium chloride (TTC) staining and fluorescent microsphere distribution (green dots) of myocardial sections 24 h after I/R. Scale bar: 2 mm. *B*) Myocardial infarction (MI) to area-at-risk (AAR) (MI/AAR) and AAR were measured after 45 min ischemia and 24 h reperfusion (Sham to *Bmp3b*$^{-/-}$, $n = 8$; WT BAT to *Bmp3b*$^{-/-}$, $n = 11$; *Bmp3b*$^{-/-}$ BAT to *Bmp3b*$^{-/-}$, $n = 12$). Values expressed as means ± SE. *C*) The level of cardiac troponin I (cTnI) was measured in plasma by ELISA 24 h after I/R injury. (Sham to *Bmp3b*$^{-/-}$, $n = 8$; WT BAT to *Bmp3b*$^{-/-}$, $n = 11$; *Bmp3b*$^{-/-}$ BAT to *Bmp3b*$^{-/-}$, $n = 12$). Values expressed as means ± SE. *P* values were determined by one-way ANOVA with Tukey correction (*B* and *C*).

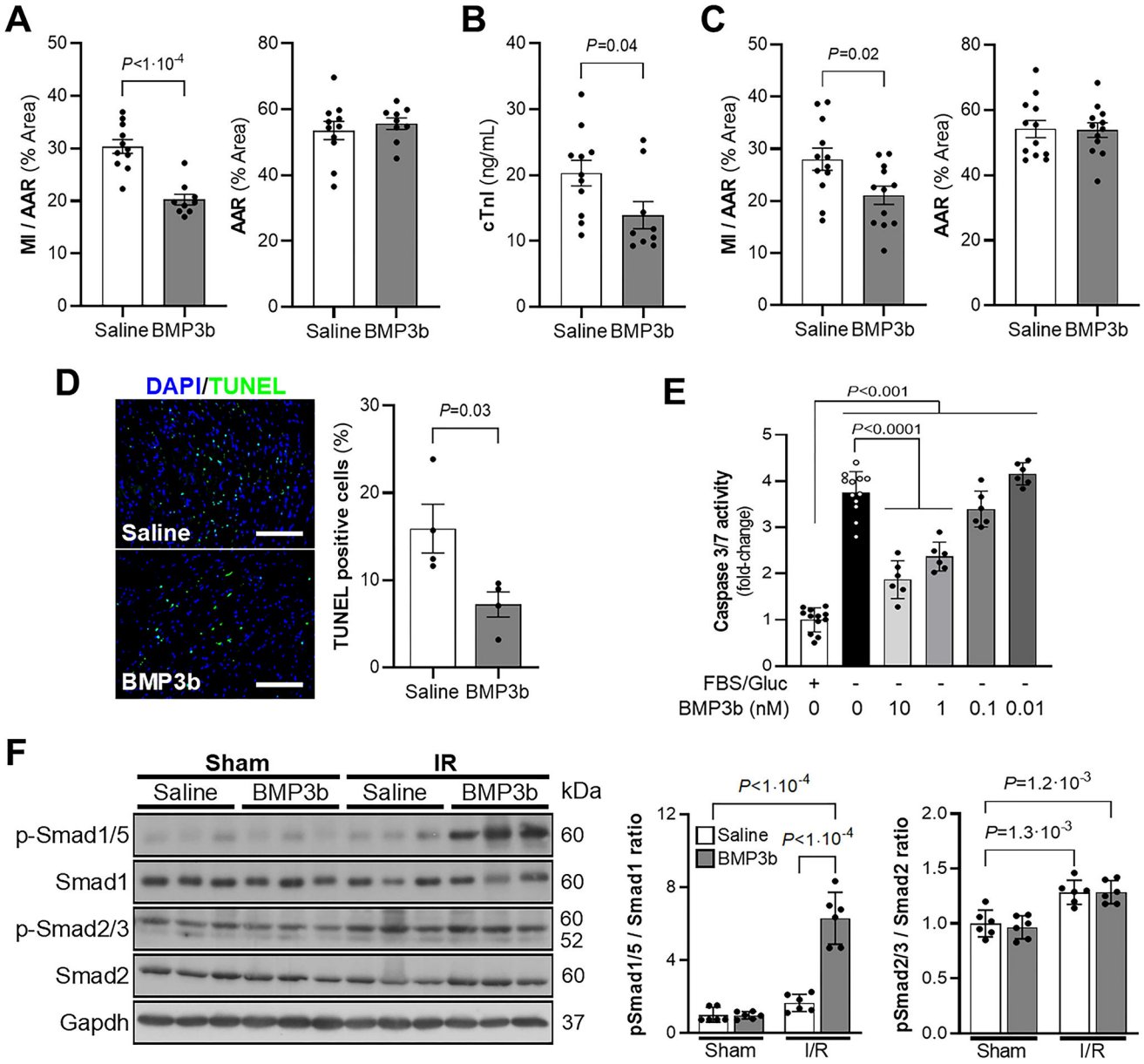

Figure 6. Treatment with BMP3b decreases myocardial infarction (MI) size in WT mice.

A) Wild-type mice were treated with saline or BMP3b (10 ng/g body weight, immediately before ischemia and the second immediately before reperfusion) and underwent I/R surgery. Heart slices were analyzed 24 h after reperfusion to obtain the ratio of (MI) to area at risk (AAR) (MI/AAR) and AAR are shown (Saline, $n = 11$; BMP3b, $n = 9$). Values expressed as means ± SE. *B)* The level of cardiac troponin I (cTnI) was measured in plasma by ELISA 24 h after I/R injury in WT mice treated with saline or BMP3b (10 ng/g body weight, immediately before ischemia and immediately before reperfusion; Saline, $n = 11$; BMP3b, $n = 9$). Values expressed as means ± SE. *C)* Wild-type mice underwent I/R surgery and were treated with saline or BMP3b (50 ng/g body weight, immediately before reperfusion). The MI/AAR ratio and AAR were analyzed 24 h after reperfusion ($n = 12$ mice each group). Values expressed as means ± SE. *D)* Representative images and quantification of TUNEL

staining on the heart sections from saline and BMP3b (10 ng/g body weight) treated mice subjected to I/R injury. (n = 4 mice each group). Values expressed as means ± SE. Scale bar: 100 μm. *E)* Caspase-3 activity was measured in rat neonatal cardiomyocytes (RNCM), starved of glucose and FBS for 2 hours and treated with the indicated concentrations of BMP3b (0 – 10nM) for 24 hours (+FBS/Gluc and –FBS/Gluc 0nM BMP3b, n=12; –FBS/Gluc 0.01 – 10nM BMP3b, n=6). Values expressed as means ± SE. *F*) Wild-type mice treated with saline or BMP3b were subjected to I/R surgery or a sham procedure. The LV was isolated 3 hours after reperfusion and the levels of SMAD1/5, and SMAD2/3 phosphorylation (p) were determined by immunoblot. Total SMAD1 and SMAD2 are also shown. Levels of GAPDH are shown as loading controls. Densitometric analysis of Western blots are shown (n = 6 mice each group). Values expressed as means ± SD. *P* values were determined by unpaired Student *t*-test (A, *B* and *C*), Mann-Whitney test (*D*), one-way ANOVA with Tukey correction (*E*) and two-way ANOVA with Tukey correction (*F*).

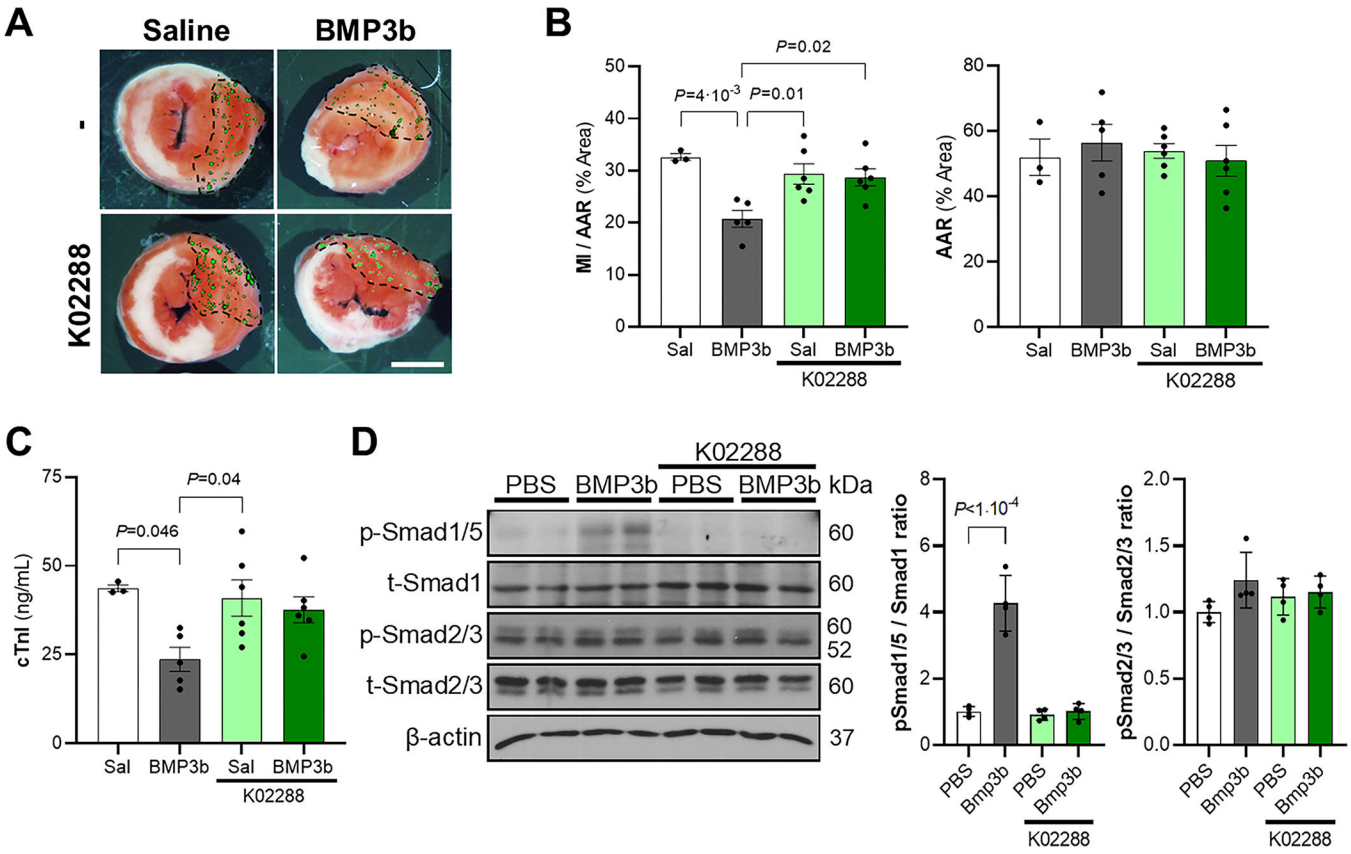

Figure 7. BMP3b cardioprotective effect occurs through the SMAD1/5 pathway.

Wild-type mice were pretreated with K02288 (3.5 mg/kg body weight, i.p.), a selective type I BMP receptor inhibitor, or saline, 1 hour before myocardial I/R surgery, and treated with BMP3b (10 ng/g body weight) or saline (Sal) immediately before ischemia and immediately before reperfusion. Myocardial sections were obtained 24 hours after reperfusion. Representative images *A*) and quantification *B)* of triphenyltetrazolium chloride (TTC) staining and fluorescent microsphere distribution (green dots) are shown. MI area and AAR from each heart section were measured. Ratio of MI to AAR (MI/AAR) and AAR are shown. (No treatment/Sal, $n = 3$; No treatment/BMP3b, $n = 5$; K02288/Sal, $n = 6$; K02288/BMP3b, $n = 6$). Values expressed as means ± SE. Scale bar: 2 mm. *C*) The level of cardiac troponin I (cTnI) was measured 24 h after reperfusion injury in the same four groups. (No treatment/Sal, $n = 3$; No treatment/BMP3b, $n = 5$; K02288/Sal, $n = 6$; K02288/BMP3b, $n = 6$). Values expressed as means ± SE. *D*) Neonatal rat cardiomyocytes were pretreated with K02288 (1μM, 30 min) or PBS, and treated with BMP3b (10nM) or PBS for 30 min. Phospho-Smad1/5 and phospho-Smad2/3 proteins levels were analyzed in cell lysates. Levels of β-actin are shown as loading control in immunoblot analysis ($n = 4$ each group). Results are expressed as means ± SD. Normality was assessed by Shapiro-Wilk test and *P* values were determined by two-way ANOVA with Tukey correction.

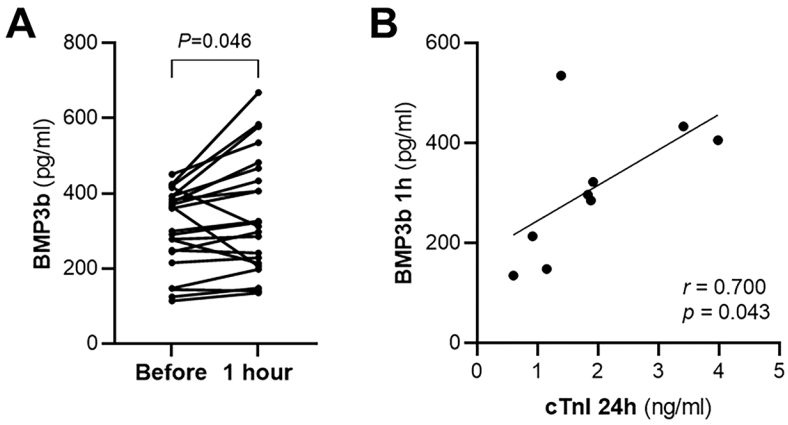

Figure 8. Human BMP3b plasmatic levels are increased after alcohol septal ablation.

A) In patients undergoing alcohol septal ablation the plasma levels of BMP3b were measured before and 1 hour after alcohol septal ablation ($n = 22$). Values are showing changes of individual subjects' data. *B*) The plasma levels of cardiac Troponin I (cTnI) were measured 24 hours after the alcohol septal ablation procedure. The correlation of cTnI measured 24 hours after the procedure and BMP3b plasma levels measured one hour after the procedure is shown ($n = 9$). *P* values were determined by paired Student *t*-test (*A*) and Spearman correlation (*B*).